Nurex Physics Manual

A.Prochazka, M.Takechi

version 1.8

Contents

1 Glauber Model

Reaction Cross Section

The total reaction cross section σ_R is calculated in Glauber model as:

$$\sigma_{\mathrm{R}} = \int [1 - T(\mathbf{b})]\, d\mathbf{b} \tag{1}$$

$$\sigma_{\mathrm{R}} = 2\pi \int b \cdot [1 - T(b)] db \tag{2}$$

where $T(b)$ is so called transparency function, b is the impact parameter, C(E) represents the Coulomb correction.

Charge Changing Cross Section

The total charge changing cross section is calculated as:

$$\sigma_{\mathrm{CC}} = \int [1 - T_{CC}(\mathbf{b})]\, d\mathbf{b} \tag{3}$$

Neutrons Removal Cross Section

The neutrons removal cross section is calculated as:

$$\sigma_{-xn} = \sigma_{\mathrm{R}} - \sigma_{\mathrm{CC}} \tag{4}$$

1.1 Phase Shift Function

The transparency functions are expressed as:

$$T(b) = e^{-2\chi(b)} \tag{5}$$

$$T_{cc}(b) = e^{-2\chi_{cc}(b)} \tag{6}$$

where $\chi_{ij}(b)$ is the phase shift function

The following two approximations are used to calculate the transparency functions:

1.1.1 Optical-limit Approximation

All four components are calculated separately, $\chi_{pp}(b), \chi_{pn}(b), \chi_{np}(b), \chi_{nn}(b)$ are the phase shift funtion for all possible proton and neutron combinations of projectile and target.

$$\chi_{ij}(b) = \int\int \Gamma_{ij}(\mathbf{b}+\mathbf{s}-\mathbf{t}, E)\cdot\rho^z_{Pi}(\mathbf{s})\cdot\rho^z_{Tj}(\mathbf{t})\, d\mathbf{s}d\mathbf{t} \tag{7}$$

where $\rho^z_{Pi}(\mathbf{s})$, $\rho^z_{Tj}(\mathbf{s})$ are z-integrated nucleon densities distribution of proton and neutrons of the projectile and the target, respectively. $\Gamma(\mathbf{b}+\mathbf{s}-\mathbf{t}, E)$ is the so-called profile function.

$$\chi(b) = \sum \chi_{ij}(b) \tag{8}$$

$$\chi_{cc}(b) = \chi_{pp}(b) + \chi_{pn}(b) \tag{9}$$

1.1.2 Modified Optical-limit Approximation

Following the procedure in [1], the Modified Optical-Limit(MOL) phase shift function is calculated as:

$$\begin{aligned}
\chi(b) = &\frac{1}{2}\int \rho^z_{Pp}(\mathbf{s})d\mathbf{s}\left(1-e^{\left(-\int\Gamma_{pp}(\mathbf{b}+\mathbf{s}-\mathbf{t})\cdot\rho^z_{Tp}(\mathbf{t})d\mathbf{t}-\int\Gamma_{pn}(\mathbf{b}+\mathbf{s}-\mathbf{t})\cdot\rho^z_{Tn}(\mathbf{t})d\mathbf{t}\right)}\right)\\
&+\frac{1}{2}\int \rho^z_{Pn}(\mathbf{s})d\mathbf{s}\left(1-e^{\left(-\int\Gamma_{pn}(\mathbf{b}+\mathbf{s}-\mathbf{t})\cdot\rho^z_{Tp}(\mathbf{t})d\mathbf{t}-\int\Gamma_{pp}(\mathbf{b}+\mathbf{s}-\mathbf{t})\cdot\rho^z_{Tn}(\mathbf{t})d\mathbf{t}\right)}\right)\\
&+\frac{1}{2}\int \rho^z_{Tp}(\mathbf{s})d\mathbf{s}\left(1-e^{\left(-\int\Gamma_{pp}(\mathbf{b}+\mathbf{s}-\mathbf{t})\cdot\rho^z_{Pp}(\mathbf{t})d\mathbf{t}-\int\Gamma_{pn}(\mathbf{b}+\mathbf{s}-\mathbf{t})\cdot\rho^z_{Pn}(\mathbf{t})d\mathbf{t}\right)}\right)\\
&+\frac{1}{2}\int \rho^z_{Tn}(\mathbf{s})d\mathbf{s}\left(1-e^{\left(-\int\Gamma_{pn}(\mathbf{b}+\mathbf{s}-\mathbf{t})\cdot\rho^z_{Pp}(\mathbf{t})d\mathbf{t}-\int\Gamma_{pp}(\mathbf{b}+\mathbf{s}-\mathbf{t})\cdot\rho^z_{Pn}(\mathbf{t})d\mathbf{t}\right)}\right)
\end{aligned} \tag{10}$$

1.1.3 Four-component MOL

To calculate MOL type calculation [1] in four components (MOL4C) the phase shift functions are calculated as:

$$\begin{aligned}
\chi_{ij}(b) = &\frac{1}{2}\int \rho^z_{Pi}(\mathbf{s})d\mathbf{s}\left(1-exp\left[-\int\Gamma_{ij}(\mathbf{b}+\mathbf{s}-\mathbf{t})\cdot\rho^z_{Tj}(\mathbf{t})d\mathbf{t}\right]\right)\\
&+\frac{1}{2}\int \rho^z_{Tj}(\mathbf{t})d\mathbf{t}\left(1-exp\left[-\int\Gamma_{ij}(\mathbf{b}+\mathbf{t}-\mathbf{s})\cdot\rho^z_{Pi}(\mathbf{s})d\mathbf{s}\right]\right)
\end{aligned} \tag{11}$$

1.1.4 Z-Integrated density

The z-integrated density is calculated using the following equations:

$$\rho_i^z(b) = \int_{-\infty}^{\infty} \rho_i(\sqrt{b^2 + z^2}) \cdot dz \tag{12}$$

in practice the integration boundaries are set to predefined maximum radius value.

$$\rho_i^z(b) = \int_{z_{min}}^{z_{max}} \rho_i(\sqrt{b^2 + z^2}) \cdot dz \tag{13}$$

1.2 Dirac Density cases

If target and projectile are both either proton or neutron the code returns the corresponding nucleus-nucleus cross section.

In cases when target or projectile is proton(or neutron) with Dirac Density function type the following equations are used to calculate phase shift function:

1.2.1 Optical Limit Approximation

$$\chi_{ij}(b) = \int\int \Gamma(\mathbf{b} + \mathbf{s} - \mathbf{t}) \cdot \rho_{P,T}^z(\mathbf{s}) \cdot \delta_{T,P}(\mathbf{t})\, d\mathbf{s}d\mathbf{t} \tag{14}$$

$$\chi_{ij}(b) = \int \Gamma(\mathbf{b} + \mathbf{s}) \cdot \rho_{P,T}^z(\mathbf{s})d\mathbf{s} \tag{15}$$

in case of Zero-Range approximation:

$$\chi_{ij}(b) = \sigma_{NN}(E) \cdot \rho_{P,i}^z(\mathbf{b}) \tag{16}$$

1.2.2 Modified Optical Limit Approximation + Finite Range

$$\chi(b) = \int \delta_T(\mathbf{t})d\mathbf{t}\left(1 - exp\left[-\int \Gamma(\mathbf{b} + \mathbf{t} - \mathbf{s}) \cdot \rho_P^z(\mathbf{s})d\mathbf{s}\right]\right) \tag{17}$$

$$\chi(b) = \left(1 - exp\left[-\int \Gamma(\mathbf{b} + \mathbf{s}) \cdot \rho_P^z(\mathbf{s})d\mathbf{s}\right]\right) \tag{18}$$

in case of Zero-Range approximation:

$$\chi(b) = \left(1 - exp\left[-\sigma_{NN}(E) \cdot \rho_P^z(\mathbf{b})\right]\right) \tag{19}$$

2 Nuclear Densities

2.1 Nuclear density definition

Input:

- A_iZ_i - Number of nucleons and the proton number of the target or projectile.
- function type and parameters.

The projectile and target nuclear densities are described in form:

$$\rho_i(\vec{r}) = f(\vec{r}, p_1, p_2, ...) \tag{20}$$

$i = t$ or p for the target and projectile density, $f(...)$ is the chosen function type. $p_1, p_2...$ are parameters of the function.

2.2 Nuclear Density Function Types

2.2.1 Fermi type

Number of free parameters = 3

$$\rho(r) = \frac{\rho_0 \cdot (1 + wr^2/c^2)}{1 + exp(\frac{|r|-c}{z})}$$

c - radius parameter , z - diffusion parameter, w - additional parameter, by default equals to zero. ρ_0 is the normalization parameter.

2.2.2 Harmonic Oscillator type (HO)

Number of free parameters = 2

$$\rho(r) = \rho_0 \cdot \left(1 + a \cdot \frac{r^2}{r_0^2}\right) \cdot exp\left(-\frac{r^2}{r_0^2}\right)$$

a - width parameter, r_0 - radius parameter, ρ_0 - normalization

2.2.3 Gaussian Type

Number of free parameters = 1

$$\rho(r) = \rho_0 \cdot exp\left(-\frac{r^2}{2 \cdot w^2}\right)$$

w - width parameter, ρ_0 - normalization

2.2.4 Dirac Type

Number of free parameters = 0

2.3 Normalization

The nuclear density functions are normalized using the normalization parameter as:

$$\int \rho_i(\vec{r}) \cdot d^3\vec{r} = A_i \tag{21}$$

$$4\pi \int r^2 \cdot \rho_i(r) \cdot dr = A_i \tag{22}$$

2.4 Root-Mean-Squared Radius

$$R^2_{rms} = \int \vec{r}^2 \rho_i(\vec{r}) \cdot d^3\vec{r} \tag{23}$$

3 Predefined nuclear densities

For certain nuclei predefined nuclear densities are available. The density function parameters are selected to reproduce the experimental root-mean-square charge radius and the saturation density of the proton and neutron distributions.

For nucleus with $A < 20$ Harmonic-Oscillator (HO) type density is used, expect proton where we use Dirac type function. For heavier nuclei the 2-parameter Fermi function is used.

The central total nucleon density is assumed to be 0.166 fm^{-3}. This density is shared between the protons and neutrons. The proton and neutron central densities are then calculated as a function of neutron excess using Equations 24, 25.

$$\rho_{0p} = 0.083042 - 0.059898 \cdot \frac{N - Z}{A} \tag{24}$$

$$\rho_{0n} = 0.166084 - \rho_{0p} \tag{25}$$

The root-mean-square radius of the proton distribu- tion were derived from the experimental charge radii measured by electron scattering and isotope-shift measurements [5].

The point-like proton radius was calculated from the experimental charge radius using [7]:

$$R^2_p = R^2_{ch} - R^2_{proton} - \frac{N}{Z} \cdot R^2_{neutron} - \frac{3\hbar^2}{4m_p^2c^2} \tag{26}$$

where R_{ch} is the experimental charge radius, R_{proton} is the mean-square charge radius of proton, $R_{neutron}$ is the mean-square charge radius of neutron and the last term is the Darwin-Foldy term.

The used values for the mean-suare charge radii of proton and neutron are $0.88 fm$ and $-0.0935 fm$, taken from [6].

The radius of the neutron distribution is then corrected for the neutron skin. The skin thickness is calculated using Eq. 27.

$$S = 0.9 \cdot \frac{N - Z}{A} - 0.03 \tag{27}$$

where S is the neutron thickness in fm unit as a function of neutron excess.

4 Profile Function

The profile function $\Gamma(\mathbf{b} + \mathbf{s} - \mathbf{t}, E)$ is parametrized as:

$$\Gamma(\mathbf{r}, E) = \frac{1}{2} \cdot \frac{1}{2\pi\beta^2} \sigma_{NN}(E) \cdot exp\left(-\frac{r^2}{2\beta^2}\right) \tag{28}$$

σ_{NN} is the nucleon-nucleon scattering cross ssection. β is the range parameter with default constant $\beta = 0.39\ fm$

Zero-Range Approximation
if $\beta = 0$

$$\Gamma(\mathbf{r}, E) = \frac{1}{2} \cdot \delta(r) \sigma_{NN}(E) \tag{29}$$

5 Nucleon-Nucleon Total Cross Sections

The σ_{NN} is taken from the measured proton-proton and proton-neutron scattering cross-sections. The parametrization is used to fit the measured data, see Figure 5.2. The in-medium effects on nucleon-nucleon scattering can be taken into account using the Fermi-motion effect, see following sections.

5.1 Fermi-motion Effect in σ_{NN}

Instead of using free nucleon-nucleon scattering cross section $\sigma_{\mathrm{NN}}(E)$, one can choose the in-medium nucleons scattering cross section ($\sigma_{\mathrm{NN}}^{\mathrm{eff}}$) which can be obtained by incorporating the Fermi motion of in-medium nucleons into the $\sigma_{\mathrm{NN}}(E)$. This option provides a good prescription to calculate cross sections in the intermediate energy region (from 30 to a few hundreds MeV/nucleon) using Glauber model.The momentum distribution of nucleons in the nucleus is assumed to be

the Gaussian according to the Goldhaber model. The momentum distribution of a projectile nucleon relative to a target nucleon parallel to the beam axis (p_{rel}) is expressed as [2]:

$$D(p_{rel}) = \frac{\exp\left(-(p_{rel} - p_{proj})^2 / 2\left(\left\langle p^2\right\rangle^P + \left\langle p^2\right\rangle^T\right)\right)}{\sqrt{2\pi\left(\langle p^2\rangle^P + \langle p^2\rangle^T\right)}}$$

Here, $\left\langle p^2\right\rangle^P$ and $\left\langle p^2\right\rangle^T$ denote the mean-square momenta of the projectile and target nucleon respectively, and p_{proj} is the momentum of a nucleon with the same velocity as the projectile nucleus. For stable nuclei, the nominal experimental value $\sqrt{\langle p^2\rangle} = 90$ MeV/c extracted from projectile-fragmentation data is assumed by default. Using Eq. (30), the momentum-averaged total cross section of nucleons in the nucleus can be written [2] as:

$$\sigma_{\mathrm{NN}}^{\mathrm{eff}} = \int_{-\infty}^{+\infty} dp_{\mathrm{rel}} \sigma_{\mathrm{NN}}(p_{\mathrm{rel}}) D(p_{\mathrm{rel}}) \tag{30}$$

5.2 Fermi Momentum from density

Fermi energy and momentum is calculated from the nucleon density function as:

$$E_f(r) = \frac{\hbar^2}{2M} \cdot (3\pi\rho(r))^{2/3} \tag{31}$$

$$p_f(r) = \sqrt{2ME_f(r)} \tag{32}$$

where $\rho(r)$ is the proton or neutron debnsity of the nucleus

To be used with the z-integrated densities, the average z-Fermi energy and momentum is calculated as:

$$E_f^z(b) = \frac{\int E_f(r)\rho_i(\sqrt{b^2 + z^2}) \cdot dz}{\int \rho_i(\sqrt{b^2 + z^2}) \cdot dz} \tag{33}$$

$$p_f^z(r) = \sqrt{2ME_f^z(r)} \tag{34}$$

The nucleon-nucleon cross section is then calculated as:

$$\sigma_{\mathrm{NN}}^{\mathrm{eff}}(E, \mathbf{t}, \mathbf{s}) = \int_{-\infty}^{+\infty} dp_{\mathrm{rel}} \sigma_{\mathrm{NN}}(p_{\mathrm{rel}}) D(p_{\mathrm{rel}}, \mathbf{t}, \mathbf{s}) \tag{35}$$

with D from Eq.30 and mean-square-momenta are not constant but calculated as:

$$\left\langle p^2\right\rangle^P(\mathbf{t}) = C_{pf} \cdot p_f^z(\mathbf{t}) \tag{36}$$

$$\left\langle p^2\right\rangle^T(\mathbf{s}) = C_{pf} \cdot p_f^z(\mathbf{s}) \tag{37}$$

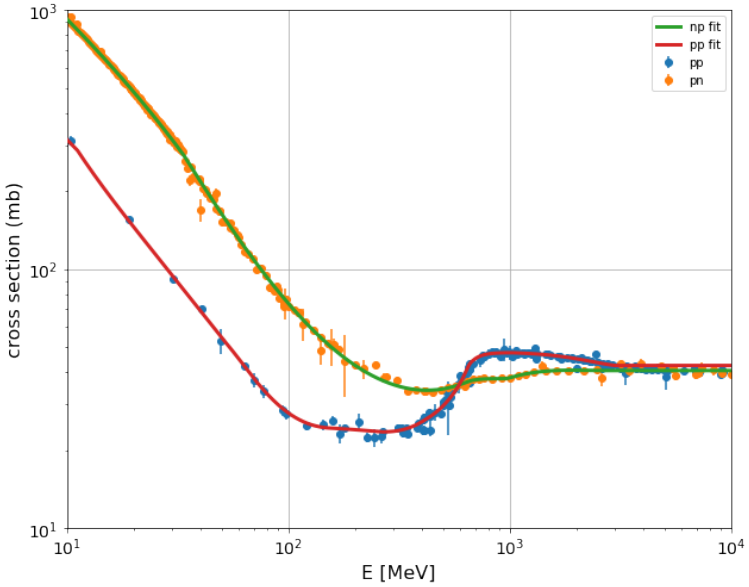

Figure 1: The measured nucleon-nucleon cross section (points) and the fit (lines) used in the library.

6 Coulomb Correction

The following Coulomb corrections are implemented in the code:

Classic correction

The cross section,ie from Eq. 1, is multiplied by the correction factor C calculated as:

$$C(E) = 1 - \frac{1.44 \cdot Z_p \cdot Z_t}{b_{max} \cdot E_{cm}} \tag{38}$$

where b_{max} is equal to $\sqrt{\sigma_R(E)/(10.0\pi)}$, σ is in mb unit.

Sommerfeld correction

The impact parameter b for the transparency function in Eq. 1 and 3 is modified as:

$$b_c = \sqrt{b^2 + d_0^2/4} + d_0/2 \tag{39}$$

b_c is Coulomb deflected impact parameter, d_0 is the closest distance at zero impact parameter, b is impact parameter at infinity

$$d_0 = 2 \cdot \eta \cdot \lambda\!\!\!^{-} = \frac{\alpha \hbar c Z_1 Z_2}{0.5 m v^2} \tag{40}$$

$\eta = \alpha Z_1 Z_2/\beta$ is the Sommerfeld parameter

7 Numerical Calculations and Precision

The NUREX code uses the Gaussian quadrature methods to calculate integrals. The type and the order of the integration can be changed at compile-time. For the adaptive quadrature we use the Gauss-Kronrod method.

The limits of the integration over the impact parameter and the radius are determined from the root-mean-squared radius of the nucleon densities. The integral 23 is calculated using the adaptive quadrature.

The z-integrated nucleon densities in profile functions, see Eq. 7, Eq. 10, are calculated at different radii and the z-integrated density is interpolated with cubic spline between the calculated points. By default the z-integrated density is calculated at 100 points between 0 and $3.5 \cdot R_{rms}$. The accuracy of z-integrated proton density of ^{12}C reconstruction is shown in Fig. 7. On the left the density and z-integrated density is shown and on the right absolute difference between interpolated and precise value is shown for multiple number if interpolate points.

In case of finite range calculation the 2-dimensional integration over the range is calculated either by using the Gauss-Hermite quadrature. The integral over range can be pre-calculated and stored in cubic splines for faster calculations. This precalculation can be disabled at compile-time. The accuracy of z- and range-integrated proton density of ^{12}C reconstruction is shown in Fig. 7. On the left the density and z-integrated density is shown and on the right absolute difference between interpolated and precise value is shown for multiple number if interpolate points.

The profile functions itself are evaluated as a cubic splines for the calculation of the cross-section, see Eq 1. The number of interpolated points can be change at the compile time. The integration in 1 and 3 is done using the adaptive quadrature.

In case of calculation with the Fermi Motion correction, the caculation of Eq. 30 depends on the limit of integration. The limits where the function is relavant are taken as $\pm 5.0 \cdot \sigma_p$. Where σ_p is squared quadratic sum of mean-square momenta of the projectile and the target, see Eq. 30. If the lower limit does not cross 0.0 to negative values Gauss-Hermite quadrature is used, otherwise in case of lower energies and bigger the slower adaptive quadrature is used.

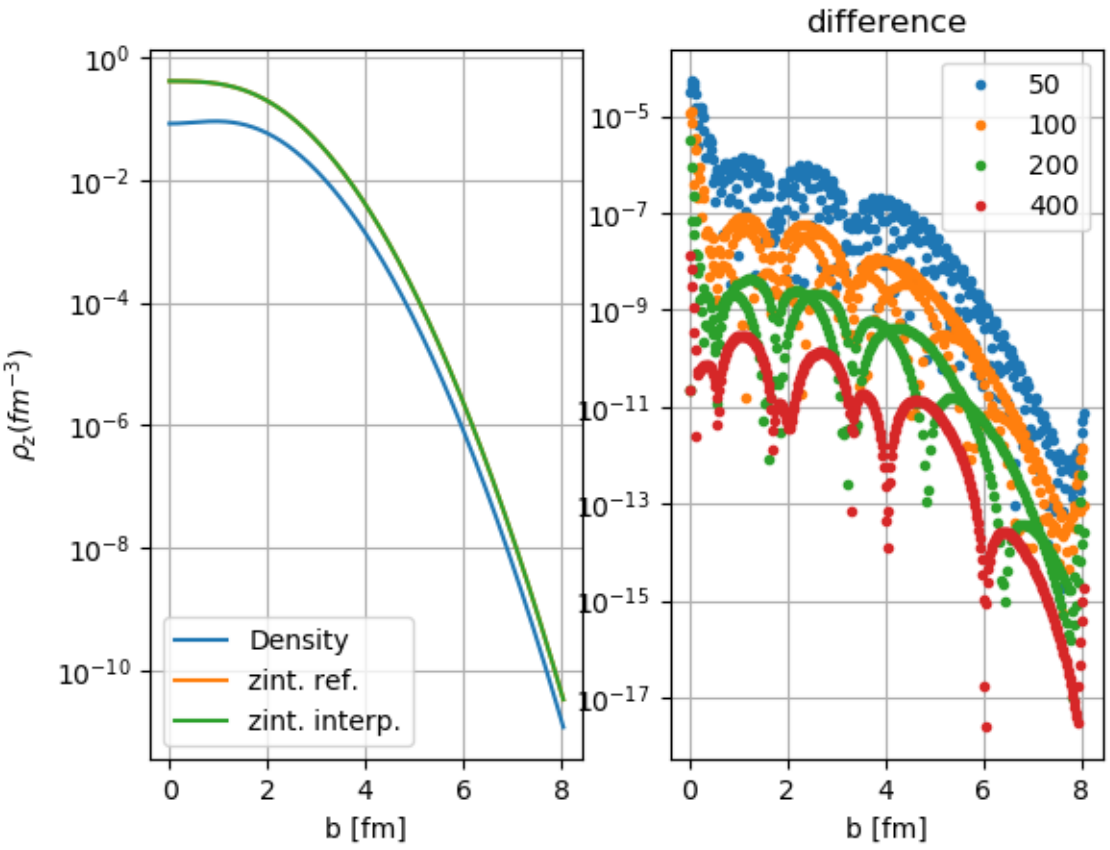

Figure 2: On the left: calculated z-integrated density (green) and density distribution(blue). On the right absolute accuracy of cubic spline interpolation and z-integration.

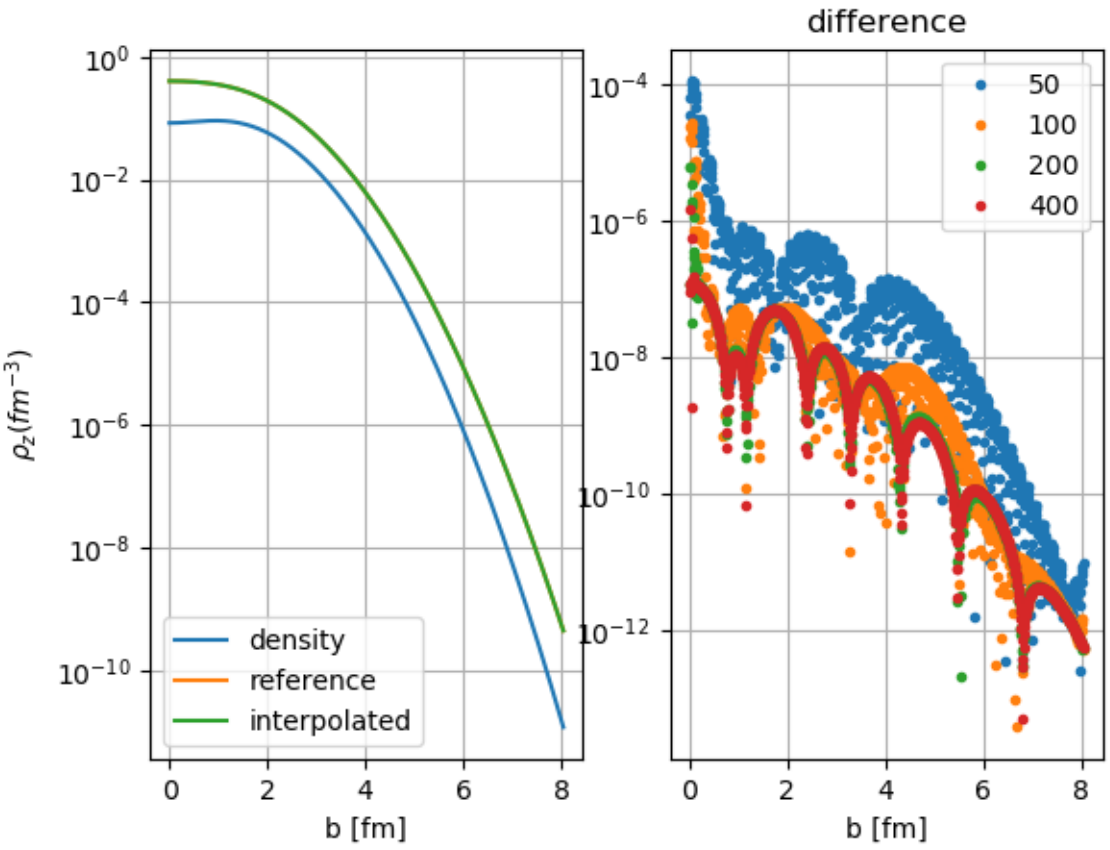

Figure 3: On the left: calculated z- and ranged-integrated density (green) and density distribution(blue). On the right absolute accuracy of cubic spline interpolation and z- + range-integration.

8 Charge-Changing Corrections

The charge-changing cross section is calculated using Eq. 3. This corresponds to the direct proton-induced reactions. To take into account indirect charge-changing reactions the following corrections are used:

- PRC82 - empirical scaling
- evaporation - neutron-induced charged particle evaporation
- none - no correction, only proton-induced part is calculated

8.1 Empirical correction factor

The measured charge-changing cross section were compared to the calculated cross sections and correction factor was estimated.

$$\sigma_{CC}(E) = \sigma_{CCp}(E) \cdot f(E) \tag{41}$$

where $f(E)$ is the correction factor, σ_{CCp} is the direct proton-induced charge-changing cross section

- PRC82 - scaling factor from [8]: $f(E) = 1.141 - 6.507 \cdot 10^{-5} \cdot E$

8.2 Charged particle evaporation correction

The indirect charge-changing reaction is assumed to be charged particle evaporation after the neutron only direct reaction.

$$\sigma_{CC} = \sigma_{CCp} + \sum_i P_{chi} \cdot \sigma_{-in} \tag{42}$$

where σ_{CC} is the total charge-changing cross section, σ_{CCp} is the direct proton-induced charge-changing cross section, P_{chi} is the charged particle evaporation probability after the i-neutrons removal reaction σ_{-in}.

8.2.1 Neutrons Removal Cross-Section

The total neutron removals are calculated from the model using Eq. 4. We assume that

$$\sigma_{-xn} = \sum \sigma_{-in} \tag{43}$$

The ratio of particular neutron removals in Eq. 42 are calculated from the Glauber model using the Eq. 44.

$$\sigma_{-in} = \binom{N_p}{i} \int b \cdot e^{-2(\chi_{pp}+\chi_{pn})} \left(e^{-2(\chi_{np}+\chi_{nn})}\right)^{N_p-i} \left(1 - e^{-2(\chi_{np}+\chi_{nn})}\right)^{i} db \tag{44}$$

where N_p is number of neutrons in projectile, i is number of removed neutrons and the profile functions are calculated using the projectile neutron density distribution normalized to 1.0.

Optionally neutron removals can be taken from the EPAX v3 parametrization [11]. The particular removals from EPAX are normalized according to the Eq. 43.

9 Particle Evaporation

9.1 Particle Evaporation Probability

$$P_e = \int_{S_e+V_b}^{\infty} \rho_{Ex}(E) w_e(E) dE \tag{45}$$

where S is the particle separation energy V_b is the particle Coulomb barrier, $\rho_{Ex}(E)$ is the excitation energy distribution and $w_e(E)$ is the probability to evaporate particle e at excitation energy E.

For the calculation of the charged-particle evaporation as used in Eq. 42 the w_e above equals to the sum of evaporation probabilities for all possible charged-particles plus probability to evaporate charge after from the residual after neutron evaporation:

$$w_{ch} = w_n \cdot w_{ch}(-n) + w_{1H} + w_{2H} + w_{3H} + w_{3He} + w_{4He} + ... \tag{46}$$

w_n and w_i are the neutron ad other particle evaporation probabilities, $w_{ch}(-n)$ is the charge evaporation probability from the residual after the neutron removal calculated using 45.

For stable and proton-rich nuclei and excitation energy above the evaporation barrier we can assume $w_{ch}(E) \approx 1.0$.

9.1.1 Excitation Energy Distribution

The excitation energy distribution is calculated using the Gaimard-Schmidt approach (optionally Ericson formula) [10]. The input parameters to the Gaimard-Schmidt formula is the maximum excitation energy E_{max} by removing a neutron and number of removed neutrons. A sample excitation distribution for $E_{max} = 40$ MeV is shown in Fig. 4. If not specified $E_{max} = 1.0 \cdot E_{fermi}(0)$ is taken, where E_{fermi} is the Fermi energy of the neutrons calculated using Eq. 31.

9.1.2 Coulomb Barrier

The particle Coulomb barrier is calculated as a maximum of a sum of the nuclear potential and Coulomb potential of charged particle and residual fragment. Tunneling through the barrier is at the moment not taken into account at the moment.

The maximum of the Coulomb barrier V_b is found numerically of the following equation:

$$V_b(r) = V_C(r) + V_N(r) \tag{47}$$

where V_C is the Coulomb potential, V_N is the nuclear potential, r is the distance between the particles.

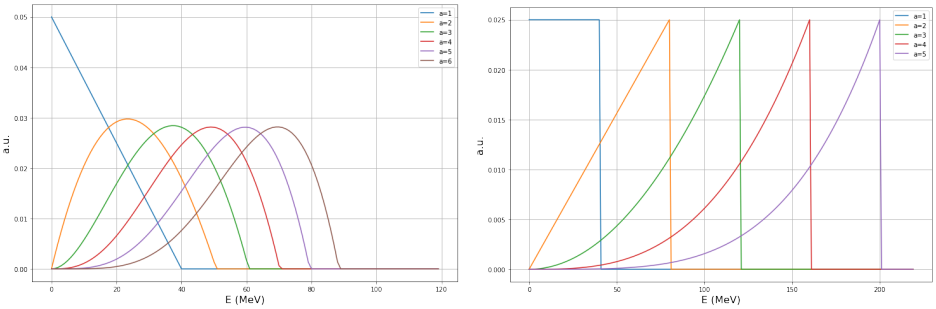

Figure 4: Prefragment excitation-energy distribution after removing a-nucleons. The maximum excitation energy E_{max} = 40MeV. On the left distribution by the Gaimard-Schmidt formula, on the right by the Ericson formula.

To speedup the calculation, alternatively to the numerical solution, the Coulomb barrier can be calculated using the parametrization as described in [18].

9.1.3 Coulomb potential

$$V_C(r) = Z_1 Z_2 e^2 \begin{cases} \frac{1}{r} & r \geq R_C \\ \frac{1}{2R_C}\left[3 - (R/R_C)^2\right] & r < R_C \end{cases}$$

where $R_C = 1.24R_1 + 1.24R_2$, where R_i is calculated by Eq. 50.

9.1.4 Nuclear potential

Bass80 model [12] is used to calculate nuclear potential

$$V_N(r) = -\frac{R_1 R_2}{R_1 + R_2}\Phi(r - R_1 - R_2) \tag{48}$$

$$\Phi(s) = \left[0.033 \cdot \exp\left(\frac{s}{3.5}\right) + 0.007 \cdot \exp\left(\frac{s}{0.65}\right)\right]^{-1} \tag{49}$$

where R_1 and R_2 are calculated as:

$$R_i = R_s\left(1 - \frac{0.98}{R_s^2}\right) fm \quad (i = 1, 2) \tag{50}$$

$$R_s = 1.28A_i^{1/3} - 0.76 + 0.8A_i^{-1/3} \tag{51}$$

9.1.5 Particle Emission Probability

To probability to evaporate charged particle at given excitation energy in eq. 45 we use the Weisskopf-Ewing formalism:

$$\Gamma_\nu = \frac{2s_\nu + 1}{2\pi\rho_i(E_x)} \frac{2m_\nu}{\pi\hbar^2} \int_0^{Ex-S-V_b} \sigma_C(\varepsilon)\rho_f(E_f) \cdot \varepsilon dE_f \tag{52}$$

where ρ_i and ρ_f are the level densities in the initial and daughter nucleus, m_ν is the mass of the evaporated particle, ε is the kinetic energy of the evaporated particle, s_ν is the spin of the evaporated particle and σ_C is the cross section of the inverse process.

The probability to evaporate particle e is then calculated as:

$$w_e(E_x) = \frac{\Gamma_e}{\sum \Gamma_i} \tag{53}$$

9.1.6 Level Density

The total level density is obtained from the Fermi-gas model for higher excitation energies and the constant-temperature model for lower excitation energies [19].

Constant-temperature model

$$\rho_{CT}(E) = \frac{\exp(\frac{E-E_0}{T})}{T} \tag{54}$$

Fermi-gas model

$$\rho_{FG}(E) = \frac{\sqrt{\pi} \cdot \exp(2\sqrt{aE_{eff}})}{12a^{1/4} \cdot E_{eff}^{5/4}} \tag{55}$$

where T is the nuclear temperature, E_0 is the energy shift, E_{eff} is the effective excitation energy, a is the level density parameter.

The effective energy E_{eff} in Eq. 55 is the excitation energy shifted due to the pairing energy ($\Delta = \Delta_p + \Delta_n$).

$$E_{eff} = E_x - \Delta \tag{56}$$

with level density parameter:

$$a = \tilde{a}\left(1 + \frac{\delta U \cdot k(E_{eff})}{E_{eff}} + \frac{\delta P \cdot h(E_{eff})}{E_{eff}}\right) \tag{57}$$

where δU is the shell correction, δP is the effective pairing shift, k is the shell energy correction damping, h is the effective pairing energy damping parameter and $\tilde{a}$ is the the asymptotic level-density paramete.

the asymptotic level-density parameter

$$\tilde{a} = 0.073A + 0.095B_sA^{2/3} \quad [MeV^{-1}] \tag{58}$$

In above B_s is the ratio of the surface of deformed nucleus to spherical nucleus surface, ie for spherical nuclei $B_s = 1$. B_s and δU are calculated from the finite range liquid-drop model [16]. The shell effect damping $k(E)$ is calculating as:

$$k(E) = 1 - \exp(-2.5\tilde{a}A^{-4/3} \cdot E) \tag{59}$$

The effective pairing energy shift δP is calculated as:

$$\delta P = -\frac{1}{4}\Delta^2 g + 2\Delta \tag{60}$$

where Δ is average pairing gap, g is single-particle level density at Fermi energy.

The pairing dumping $h(E) = 1 - (1 - E/E_{crit})$ for $E < E_{crit}$ otherwise $h(E) = 1$

9.1.7 Angular Momentum Factor

The angular momentum factor for level density with given spin is:

$$g_J(J) = \frac{2J+1}{\sqrt{8\pi}\sigma^3} \exp\left(-\frac{(J+1/2)^2}{2\sigma^2}\right) \tag{61}$$

where $\rho_{intr}(E)$ is the level density of intrinsic excitation, $K_{coll}(E)$ is the collective enhancement factor.

For the level density including all spins:

$$g_J(J) = \frac{1}{\sqrt{2\pi}\sigma} \tag{62}$$

and including all magnetic quantum numbers:

$$g_J(J) = 1 \tag{63}$$

σ^2 is the spin cutoff parameter:

$$\sigma^2 = \frac{JT}{\hbar^2} \tag{64}$$

T is the nuclear temperature

9.1.8 Rotational enhancement

For nuclei with quadrupole deformation $|\beta_2| \geq 0.15$ the rotational enhancement is calculated as [15]:

$$K_{rot}(E_{corr}) = \begin{cases} (\sigma_\perp^2 - 1) f(E) & \sigma_\perp^2 > 1 \\ 1 & \sigma_\perp^2 \leq 1 \end{cases}$$

$$f(E_{corr}) = \left(1 + \exp\left(\frac{E_{corr} - E_{cr}}{d_{cr}}\right)\right)^{-1} \tag{65}$$

where $E_{cr} = 40MeV$ and $d_{cr} = 10MeV$.

$$\sigma_\perp^2 = \frac{J_\perp T}{\hbar^2} \tag{66}$$

where $J_\perp$ is the moment of inertia perpendicular to the symmetry axis.

For $|\beta_2| < 0.15$ the vibrational enhancement is calculated using the above equations, but spin-cutoff parameter $\sigma_\perp^2$ is modified as: $\sigma_\perp^{2`} = 75 * \beta_{eff} * \sigma_\perp^2$ [17]. Here the deformation parameter $\beta_{eff} = 0.022 + 0.003\Delta N + 0.0005\Delta Z$ [15]. ΔZ and ΔN are absolute number of protons and neutrons above or bellow closest shell closure.

Nuclear level densities are expressed as[15]:

$$\rho(E) = K_{coll}(E) g_J(J) \rho_{intr}(E) \tag{67}$$

9.1.9 Inverse Cross Section

At excitation energies above the evaporation barrier the inverse cross section is calculated as [17]:

$$\sigma_C = \pi (R_{geom} + R_\alpha)^2 (1 - \frac{V_b}{\varepsilon}) \tag{68}$$

$$R_{geom} = 1.16(A_d^{1/3} + A_p^{1/3}) \tag{69}$$

$$R_\alpha = \sqrt{\frac{\hbar^2}{2\mu E_{cm}}} \tag{70}$$

where μ is the relative mass and $E_{cm} = \varepsilon(A_d - A_p)/A_d$

10 Nucleon-Nucleon Total Cross Sections Parametrization

10.1 Proton-Proton Total Cross Sections

Kinetic Energy E < 1 MeV

$$\sigma_{pp}(E) = 0.0$$

Kinetic Energy 1 MeV ≤ E < 1.5 MeV

$$\sigma_{pp}(E) = (-503.08 + 4761.3 \cdot E^{-0.49562})/2.917$$

Kinetic Energy 1.5 MeV ≤ E < 2.5 MeV

$$\begin{aligned}\sigma_{pp}(E) = &((-503.08 + 4761.3 \cdot E^{-0.49562})/2.917) \cdot (2.5 - E) \\ &+ (\exp[8.3738 - 0.63495(\log E) + 0.14901(\log E)^2 - 0.1317(\log E)^3 \\ &+ 0.033962(\log E)^4 - 0.0034031(\log E)^5]) \cdot (E - 1.5)\end{aligned}$$

Kinetic Energy 2.5 MeV ≤ E < 11.05 MeV

$$\begin{aligned}\sigma_{pp}(E) = &\exp[8.3738 - 0.63495(\log E) + 0.14901(\log E)^2 \\ &- 0.1317(\log E)^3 + 0.033962(\log E)^4 - 0.0034031(\log E)^5]\end{aligned}$$

Kinetic Energy 11.05 MeV ≤ E < 50 MeV

$$\begin{aligned}\sigma_{pp}(E) = &\exp[13.257 - 5.832(\log E) + 1.2461(\log E)^2 \\ &+ 0.07779(\log E)^3 - 0.074157(\log E)^4 + 0.0078546(\log E)^5]\end{aligned}$$

Kinetic Energy 50 MeV ≤ E < 70 MeV

$$\begin{aligned}\sigma_{pp}(E) = &(\exp[13.257 - 5.832(\log E) + 1.2461(\log E)^2 \\ &+ 0.07779(\log E)^3 - 0.074157(\log E)^4 + 0.0078546(\log E)^5]) \cdot \frac{70 - E}{20} \\ &+ (\exp[43.793 - 31.3(\log E) - 2.2222(\log E)^2 \\ &- 2.308(\log E)^3 + 0.5649(\log E)^4 - 0.037926(\log E)^5]) \cdot \frac{E - 50}{20}\end{aligned}$$

Kinetic Energy 70 MeV ≤ E < 150.37 MeV

$$\sigma_{pp}(E) = \exp[43.793 - 31.3(\log E) - 2.2222(\log E)^2 - 2.308(\log E)^3 + 0.5649(\log E)^4 - 0.037926(\log E)^5]$$

Kinetic Energy 150.37 MeV ≤ E < 260.87 MeV

$$\sigma_{pp}(E) = 0.0076434 + 25.5503$$

Kinetic Energy 260.87 MeV ≤ E < 411.97 MeV

$$\sigma_{pp}(E) = \exp[-8.5816 + 3.3171(\log E) + 0.29625(\log E)^2 - 0.056291(\log E)^3 - 0.024141(\log E)^4 + 0.0031779(\log E)^5]$$

Kinetic Energy 411.97 MeV ≤ E < 600 MeV

$$\sigma_{pp}(E) = 20.826 + 0.49428\exp[-0.0057621 \cdot E]$$

Kinetic Energy 600 MeV ≤ E < 680 MeV

$$\sigma_{pp}(E) = (20.826 + 0.49428\exp[-0.0057621 \cdot E]) \cdot \frac{680 - E}{80} + (47.614 - 125110\exp[-0.015477 \cdot E]) \cdot \frac{E - 600}{80}$$

Kinetic Energy 680 MeV ≤ E < 1000 MeV

$$\sigma_{pp}(E)47.614 - 125110\exp[-0.015477 \cdot E]$$

Kinetic Energy 1000 MeV ≤ E ≤ 3000 MeV

$$\sigma_{pp}(E) = 45.847 + 0.0052698E - 0.000041863E^2 + 6.8537 * 10^{-10}E^3$$

Kinetic Energy E > 3000 MeV

$$\sigma_{pp}(E) = \sigma_{pp}(3000)$$

10.2 Proton-Neutron Total Cross Sections

Kinetic Energy E < 0.00882 MeV

$$\sigma_{pn}(E) = 20360$$

Kinetic Energy 0.00882 ≤ E < 0.0505 MeV

$$\sigma_{pn}(E) = -160030 + 168000 \cdot E^{-0.02494}$$

Kinetic Energy 0.0505 ≤ E < 0.2 MeV

$$\sigma_{pn}(E) = -163380 + 166200 \cdot E^{-0.02494}$$

Kinetic Energy 0.2 ≤ E < 0.38 MeV

$$\begin{aligned}\sigma_{pn}(E) = (-163380 + 166200 \cdot E^{-0.02494}) \cdot \frac{0.38 - E}{0.18} \\ +(-503.08 + 4761.3E^{-0.49562}) \cdot \frac{E - 0.2}{0.18}\end{aligned}$$

Kinetic Energy 0.38 ≤ E < 1.5479 MeV

$$\sigma_{pn}(E) = -503.08 + 4761.3E^{-0.49562}$$

Kinetic Energy 1.5479 ≤ E < 2.0 MeV

$$\begin{aligned}\sigma_{pn}(E) = (-503.08 + 4761.3E^{-0.49562}) \cdot \frac{2 - E}{0.4521} \\ + \\ (\exp[8.3738 - 0.63495(\log E) \\ + 0.14901(\log E)^2 - 0.1317(\log E)^3 \\ - 0.033962(\log E)^4 + 0.0034031(\log E)^5]) \cdot \frac{E - 1.5479}{0.4521}\end{aligned}$$

Kinetic Energy 2 MeV ≤ E < 34

$$\begin{aligned}\sigma_{pn}(E) = \exp[8.3738 - 0.63495(\log E) \\ + 0.14901(\log E)^2 - 0.1317(\log E)^3 \\ - 0.033962(\log E)^4 + 0.0034031(\log E)^5]\end{aligned}$$

Kinetic Energy 34 MeV ≤ E < 598

$$\begin{aligned}\sigma_{pn}(E) = \exp[&7.8594 + 1.291(\log E) \\ &- 0.95228(\log E)^2 + 0.13433(\log E)^3 \\ &- 0.0057926(\log E)^4 + 0.000092646(\log E)^5]\end{aligned} \tag{71}$$

Kinetic Energy 598 MeV ≤ E < 700

$$\begin{aligned}\sigma_{pn}(E) = (\exp[&7.8594 + 1.291(\log E) \\ &- 0.95228(\log E)^2 + 0.13433(\log E)^3 \\ &- 0.0057926(\log E)^4 + 0.000092646(\log E)^5]) \cdot \frac{700 - E}{102} \\ &+ \\ (\exp[&-112.96 + 25.957(\log E) \\ &+ 1.0306(\log E)^2 - 0.086902(\log E)^3 \\ &- 0.09889(\log E)^4 + 0.0090234(\log E)^5]) \cdot \frac{E - 598}{102}\end{aligned}$$

Kinetic Energy 700 MeV ≤ E < 981.18

$$\begin{aligned}\sigma_{pn}(E) = \exp[&-112.96 + 25.957(\log E) \\ &+ 1.0306(\log E)^2 - 0.086902(\log E)^3 \\ &- 0.09889(\log E)^4 + 0.0090234(\log E)^5]\end{aligned}$$

Kinetic Energy 981.18 MeV ≤ E ≤ 2500

$$\begin{aligned}\sigma_{pn} = \exp[&-7.3768 + 0.43052(\log E) \\ &+ 0.4123(\log E)^2 + 0.037464(\log E)^3 \\ &- 0.018571(\log E)^4 + 0.0011638(\log E)^5]\end{aligned}$$

Kinetic Energy E ≤ 2500

$$\sigma_{pn}(E) = \sigma_{pn}(2500)$$

11 Comparison with the experimental data

We benchmarked models against various experimental data from projectile energy of 30 MeV/u. To choose the best combination of model and corrections we use the

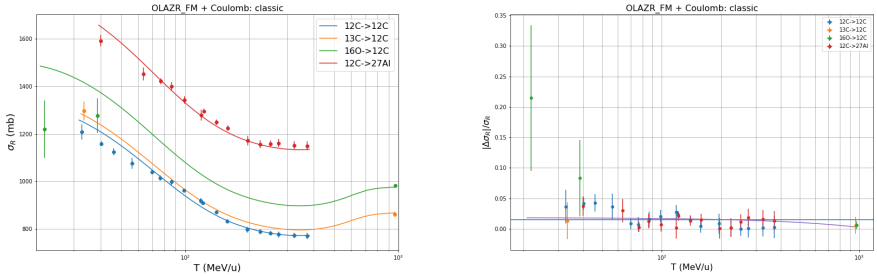

Figure 5: Benchmark of the total reaction cross section calculation against experimental data for light stable nuclei. OLA model with Zero Range approximation and Fermi motion and Coulomb corrections was used. Average deviation is 1.5%

following quantities to estimate how good the model reproduce the experimental data.

$$\Delta = \frac{|\sigma_{exp} - \sigma_{gm}|}{\sigma_{exp}} \tag{72}$$

$$\chi^2_v = \frac{\sum(\sigma_{exp} - \sigma_{gm})^2}{v} \tag{73}$$

11.1 Total Reaction Cross-Section

The models are compared with the experimental data for light stable and neutron-rich nuclei. Data are taken from [2], [3] [13], [14]

11.1.1 Optical Limit Approximation Model

The Optical Limit Approximation (OLA) model with Zero Range approximation and with Fermi Motion and Coulomb corrections for light stable nuclei with the relative deviation is shown in Fig. 5 and for neutron-rich ^8Li in Fig. 6. The average deviation calculated by Eq. 72 is 1.5% over whole range of projectile energy.

References

[1] B. Abu-Ibrahim and Y. Suzuki, PRC61(2000)051601

[2] M. Takechi et al., PRC79(2009)061601

[3] S. Kox et al., PRC35

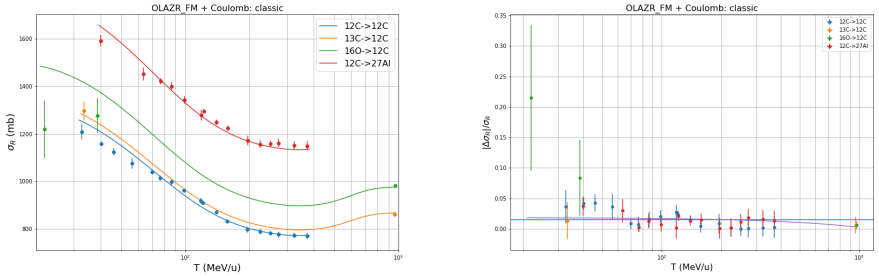

Figure 6: Benchmark of the total reaction cross section calculation against experimental data for ^{8}Li. OLA model with Zero Range approximation and Fermi motion and Coulomb corrections was used. Average deviation is 1.2%

[4] A. Ozawa et al., NPA691 (2001)

[5] I. Angeli and K.P. Marinova, Atomic and Nuclear Data Tables 99(2013)

[6] P.J. Mohr et al., Journal of Phys. and Chem. Ref. Data 45(2016)

[7] T. Yamaguchi et al., PRL107(2011)032502

[8] T. Yamaguchi et al., PRC82(2010)

[9] M. Tanabashi et al. (Particle Data Group), Phys. Rev. D 98, 030001 (2018).

[10] J.-J. Gaimard et al, Nucl. Phys A531(1991)709

[11] K. Suemmerer, Phys. Rev. C86(2012)014601

[12] R. Bass, Lecure Notes in Physics 117 (1980)

[13] G. W. Fan et al., Phys. Rev. C. 90(2014)

[14] I. Tanihata et al., Phys. Rev. Let. 55(1985)

[15] A.R. Junghans et al., Nucl. Phys. A629(1998)635

[16] P. Moöller et al., Atomic and Nuclear Data Tables,

[17] A. Kelic et al., ABLA07, Arxiv

[18] R. Kumari, CJP000 (2017) 1-8

[19] A. Gilbert, A. G. W. Cameron, Can. J. Phys. 43(1965)